ACS Macro Letters

Letter

pubs.acs.org/macroletters

Effect of the Hydrophilic Component in Aromatic Ionomers: Simple Structure Provides Improved Properties as Fuel Cell Membranes

Junpei Miyake,[†] Takashi Mochizuki,[‡] and Kenji Miyatake*[,†,§]

[†]Clean Energy Research Center, [‡]Interdisciplinary Graduate School of Medicine and Engineering, and [§]Fuel Cell Nanomaterials Center, University of Yamanashi, 4 Takeda, Kofu 400-8510, Japan

Supporting Information

ABSTRACT: To elucidate the effect of the hydrophilic component on the properties of aromatic ionomers, we have designed for the first time one of the simplest possible structures, the sulfo-1,4-phenylene unit, as the hydrophilic component. A modified Ni-mediated coupling polymerization produced the title aromatic ionomers composed of sulfonated *p*-phenylene groups and oligo(arylene ether sulfone ketone)s, as high-molecular-weight polymers (M_w = 202−240 kDa), resulting in the formation of tough, flexible membranes. The aromatic ionomer membranes showed well-developed hydrophilic/hydrophobic phase separation. Comparison with our previous aromatic ionomer membrane containing sulfonated benzophenone groups as a hydrophilic component revealed that the simple sulfophenylene structure (i.e., no polar groups such as ether, ketone, or sulfone groups in the hydrophilic component) was effective for the improvement of the membrane properties, i.e., reduced water uptake and excellent mechanical stability under humidified conditions. Furthermore, because of the high local ion exchange capacity (IEC), the simple structure led to high proton conductivity, especially at low humidity (reaching up to ca. 7.3 mS/cm at 80 °C and 20% RH), which is one of the highest values reported thus far. The improved properties of the membranes were also confirmed in an operating fuel cell.

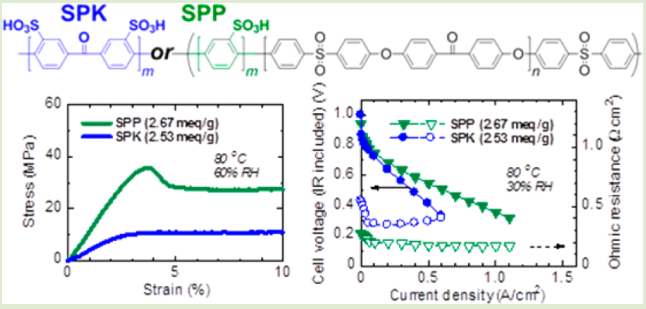

Aromatic ionomers with acidic functions have been extensively investigated for applications such as batteries, electrolyzers, fuel cells, and sensors. Considerable effort has been devoted during the last two decades to develop proton-conductive aromatic polymers for fuel cell applications, as alternatives to state-of-the-art perfluorinated ionomer membranes such as Nafion.[1−5] Fluorine-free aromatic polymers are attractive in terms of high thermal stability, low gas permeability, environmental compatibility, and cost effectiveness. Such polymers include sulfonated poly(arylene ether)s,[6−9] polyimides,[10−12] polyphenylenes,[13−16] and others.[17−19] It has been demonstrated that polymer electrolyte membranes (PEMs) composed of sulfonated and unsulfonated blocks are much more proton-conductive than the random copolymer equivalents because the former are likely to form well-developed hydrophilic/hydrophobic phase separation with interconnected ionic channels.[20] We have developed segmented copolymers composed of highly sulfonated benzophenone groups as hydrophilic components.[21] The segmented copolymer (SPK-*bl*-1, Scheme 1b) membranes are highly proton-conductive, comparable to Nafion membranes over a wide range of humidity. In order to achieve high performance, most aromatic ionomer membranes (including our SPK-*bl*-1) need relatively high ion exchange capacity (IEC), which causes large water uptake and swelling under fully hydrated conditions and may cause mechanical failure.

Most of the properties of aromatic ionomers as PEMs are associated with their hydrophilic components since acid groups absorb water as a plasticizer, and the hydrated protons take part in proton conduction. In our quest to develop better performing aromatic ionomers, we came upon the idea of applying one of the simplest possible structures, the sulfophenylene group, as the hydrophilic component. Sulfophenylene main chains with no heteroatom linkages (e.g., ether, ketone, sulfone) are expected to provide ionomer membranes with good mechanical and chemical stabilities. In addition, such a simple molecular design leads to high IEC values in the hydrophilic segments (i.e., local IEC), which we reasoned might contribute to the improvement of proton conductivity. Sulfophenylene main chains can be achieved by a conventional polycondensation reaction of the commercially available monomer (2,5-dichlorobenzenesulfonic acid), which to the best of our knowledge has not been examined for this purpose. In this paper, we report on aromatic ionomers containing sulfophenylene groups as hydrophilic components. The effects of this simple hydrophilic component on proton conductivity, mechanical properties, and fuel cell performance are discussed. The properties of the copolymer membranes are compared with those of the SPK-*bl*-1 membrane.

The title segmented copolymers **3** were synthesized from monomer **1** and oligomer **2**[21] (n = 5) via a Ni-mediated

Received: June 8, 2015
Accepted: June 30, 2015
Published: July 2, 2015

DOI: 10.1021/acsmacrolett.5b00385
ACS Macro Lett. 2015, 4, 750−754

Scheme 1. (a) Synthesis of Title Segmented Copolymer (3) and (b) Chemical Structure of Reference Polymer (SPK-*bl*-1)

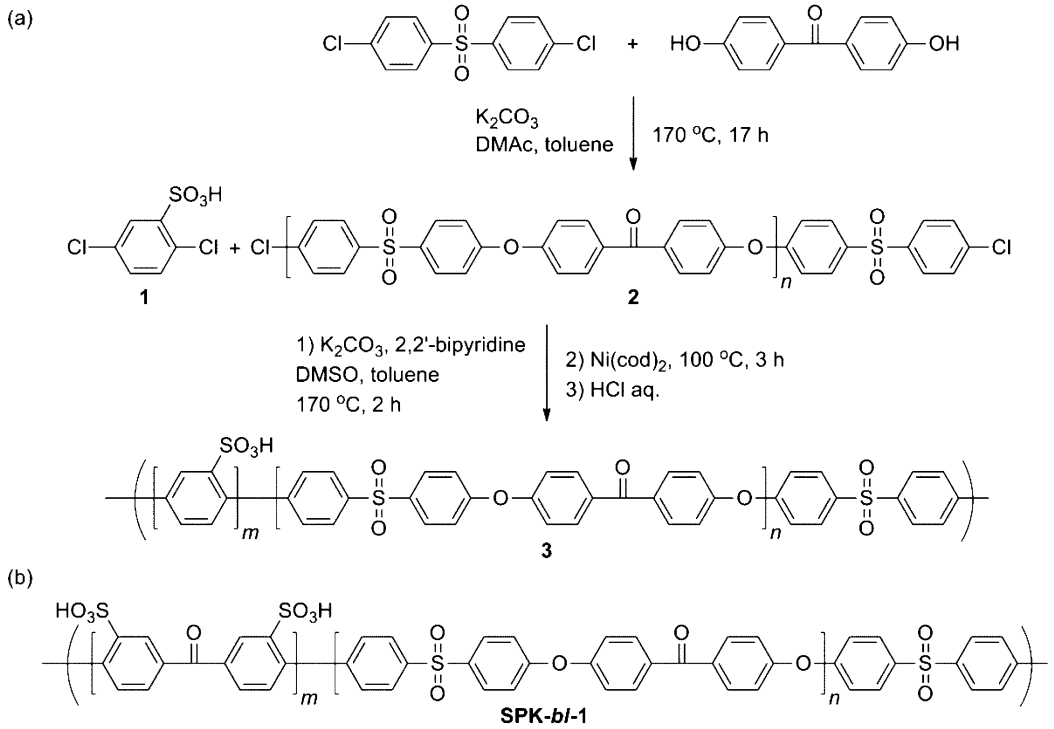

coupling reaction (Scheme 1a). It should be noted that the addition of K_2CO_3 (to neutralize the sulfonic acid groups of monomer **1**) in this polymerization system was crucial; i.e., the polymerizations with K_2CO_3 provided copolymers **3** having much higher molecular weights (M_w = 202−240 kDa) than that obtained without K_2CO_3 (M_w = 90 kDa). Two samples of **3** were prepared by changing the feed comonomer ratio (Table 1). Both polymers were soluble in polar aprotic solvents such as DMSO and were characterized by ^{1}H NMR spectra. In the ^{1}H NMR spectra of **3b** (Figure S1, Supporting Information), the peaks at ca. 8.2−8.4, 7.9, and 7.4−7.5 ppm were assigned to the sulfo-2,5-phenylene groups, and the peaks at ca. 7.2, 7.8, and 8.0 ppm were assigned to the hydrophobic blocks. The results suggest successful formation of the targeted segmented copolymer. Both samples provided self-standing, flexible **3** membranes by solution casting. While the IEC values obtained from ^{1}H NMR spectra and titration of the **3** membranes were in good agreement, they were smaller than the targeted values (Table 1), mostly because of the lower reactivity of the sulfonated monomer **1** than the hydrophobic oligomer **2** under the given polymerization conditions.

Table 1. IECs, Compositions, and Molecular Weights of 3

	IEC[a] (meq/g)	IEC[b] (meq/g)	IEC[c] (meq/g)	m/n[d]	M_n[e] (kDa)	M_w[e] (kDa)
3a	2.58	1.77	1.78	5/5	24	202
3b	3.60	2.43	2.67	10/5	22	240

[a]Calculated from the feed comonomer ratio. [b]Determined by ^{1}H NMR spectra. [c]Determined by titration. [d]Determined by the titrated IEC values when n = 5. [e]Determined by GPC analyses (calibrated with polystyrene standards).

As observed in the TEM image (Figure S2, Supporting Information), the **3b** membrane (2.67 mequiv/g), after being stained with lead ions exhibited phase-separated morphology based on hydrophilic (black) domain and hydrophobic (white) domain differences, which is similar or somewhat less pronounced compared to that of our previous segmented copolymer SPK-*bl*-1, sharing the same hydrophobic blocks.[21] The size of the hydrophobic domains and the hydrophilic domains was ca. 10 nm in width and ca. 5 nm in width, respectively.

Figure 1 compares the humidity dependence of the water uptake and proton conductivity of the **3**, SPK-*bl*-1, and Nafion NRE212 membranes at 80 °C. The water uptake of the **3**

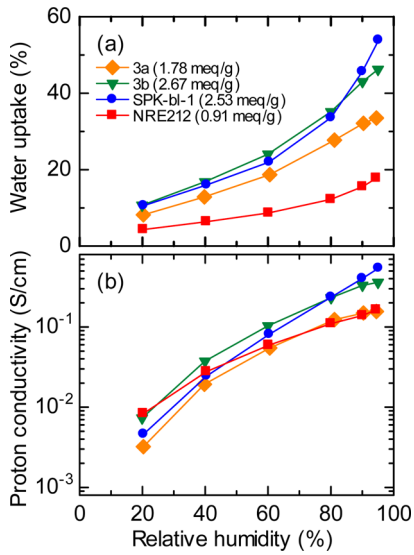

Figure 1. Humidity dependence of (a) water uptake and (b) proton conductivity of **3a** (1.78 mequiv/g, orange diamonds), **3b** (2.67 mequiv/g, green inverted triangles), SPK-*bl*-1 (2.53 mequiv/g, blue circles), and Nafion NRE212 (0.91 mequiv/g, red squares) membranes at 80 °C.

DOI: 10.1021/acsmacrolett.5b00385
ACS Macro Lett. 2015, 4, 750−754

membranes followed the order of the IEC values at all relative humidities (RH). While the high-IEC **3b** (2.67 mequiv/g) and SPK-*bl*-1 (2.53 mequiv/g) membranes showed similar water uptake values at <80% RH, a larger increase in the water uptake was observed for SPK-*bl*-1 at humidities higher than 80% RH.

In other words, the **3** membranes did not absorb excess water even under such highly humidified conditions (e.g., 80 °C and >80% RH). There are two plausible reasons for this suppression of the water uptake at high RH for the **3** membranes: (1) stronger intermolecular interactions due to the linear, highly symmetrical 1,4-phenylene backbone (Figure S3, Supporting Information) and (2) lower water affinity due to the lack of polar groups such as the carbonyl groups in SPK-*bl*-1. SPK-*bl*-1 membranes with lower IEC values also showed similar water uptake behavior (Figure S4, Supporting Information), supporting the idea that the existence of the carbonyl groups in the SPK-*bl*-1 membranes may account for the excess water absorption at high RH.

The proton conductivity was somewhat more complex, which seemed dependent not only on the water uptake but also on the chemical structure of the hydrophilic segments. In the high RH regions (ca. >50% RH), the water uptake determined the order of the proton conductivity; e.g., at ca. 95% RH, the SPK-*bl*-1 membrane (54% water uptake) showed higher proton conductivity (543 mS/cm) than that (360 mS/cm) of the **3b** membrane (46% water uptake). On the other hand, in the low RH regions (ca. <50% RH), the difference in the chemical structure of the hydrophilic components seemed to be dominant, i.e., at ca. 20% RH, the **3b** membrane (sulfophenylene groups) exhibited higher proton conductivity (7.3 mS/cm) than that (4.6 mS/cm) of the SPK-*bl*-1 membrane (sulfonated benzophenone groups) despite their similar water uptake and IEC values (Figure 1). Taking the possible sequential (block-like) structure of the sulfophenylene unit in the **3** membranes into account, the higher proton conductivity of **3b** compared to that of SPK-*bl*-1 might have resulted from the difference in the local IEC values (ion concentration); i.e., the higher local IEC value of **3** (6.40 mequiv/g) than that of SPK-*bl*-1 (5.88 mequiv/g) may have contributed to the higher proton conductivity of **3** at low RH. Furthermore, it should be noted that the **3b** membrane showed comparable or higher proton conductivity than that of the state-of-the-art Nafion NRE212 membrane at all RH. In addition, the **3b** membrane exhibited high proton conductivity even at high temperature, e.g., 55 mS/cm at 120 °C and 50% RH (Figure S5, Supporting Information), which was comparable to that of SPK-*bl*-1 (Figure S6, Supporting Information). Although the water uptake decreased with increasing temperature, the proton conductivity showed nearly the same values. This result indicates that the lower water content at 120 °C was probably countervailed by the increased mobility of the hydronium ions.

The suppression of the excess water uptake at high RH in the **3** membranes had a significant impact on the mechanical properties under humidified conditions. Figure 2 shows the storage modulus (E'), loss modulus (E''), and tan δ (E'/E'') of the membranes at 80 °C as a function of RH. The **3** membranes showed excellent viscoelastic properties with slight dependence on RH, i.e., slight decrease in E' with increasing RH, and no transitions in E'' and tan δ curves at all RH. This result is in contrast to the case of the SPK-*bl*-1 membrane, in which a drop in E' and clear transition (possible glass transition) in E'' and tan δ curves were observed at ca. 60% RH. The **3** membranes retained E' values higher than 1 GPa,

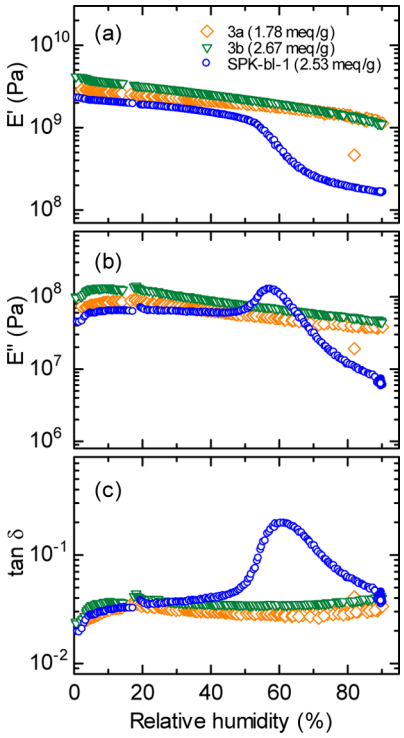

Figure 2. Humidity dependence of (a) storage modulus (E'), (b) loss modulus (E''), and (c) tan δ (E'/E'') curves of **3a** (1.78 mequiv/g, orange diamonds), **3b** (2.67 mequiv/g, green inverted triangles), and SPK-*bl*-1 (2.53 mequiv/g, blue circles) membranes at 80 °C.

even under humidified conditions. The **3b** membrane with higher IEC value (2.67 mequiv/g) showed higher E' values at low RH (ca. 4 GPa) than that of the **3a** with lower IEC value (ca. 3 GPa), indicating that the increase in the rigid sulfo-1,4-phenylene segment (Table 1 and Figure S3, Supporting Information) may contribute to an increase in E' values despite the higher water uptake.

The high mechanical stability of the **3** membranes under humidified conditions was further confirmed by tensile tests at 80 °C and 60% RH by a universal testing instrument (Figure 3). Even under such humidified conditions, the **3** membranes possessed a high initial Young's modulus (>1 GPa), maximum stress at the break point (>30 MPa), and reasonable strain (>66%) (Table S1, Supporting Information) due to the coexistence of relatively flexible oligo(arylene ether sulfone ketone) moieties and highly rigid sulfo-1,4-phenylene segments. In contrast, the SPK-*bl*-1 membrane showed a much lower Young's modulus (<0.5 GPa) than those of the **3** membranes, which is in accordance with the DMA results mentioned above.

A membrane electrode assembly (MEA) was prepared from the **3b** (2.67 mequiv/g) membrane and subjected to fuel cell performance tests. The fuel cell performance of the **3b** cell was compared with that of an SPK-*bl*-1 (2.53 mequiv/g) cell under the same operating conditions.[22] Figure 4 shows polarization curves (ohmic (*IR*) drop-included) and ohmic resistances. The open circuit voltage (OCV) was 0.972 V for the **3b** cell and 0.970 V for the SPK-*bl*-1 cell at 100% RH, suggesting good gas barrier properties of the membranes. While the two cells showed comparable cell voltages and ohmic resistances at 100% RH (Figure 4a), the **3b** cell showed much better fuel cell performance than that of the SPK-*bl*-1 cell at 30% RH (Figure

DOI: 10.1021/acsmacrolett.5b00385
ACS Macro Lett. 2015, 4, 750−754

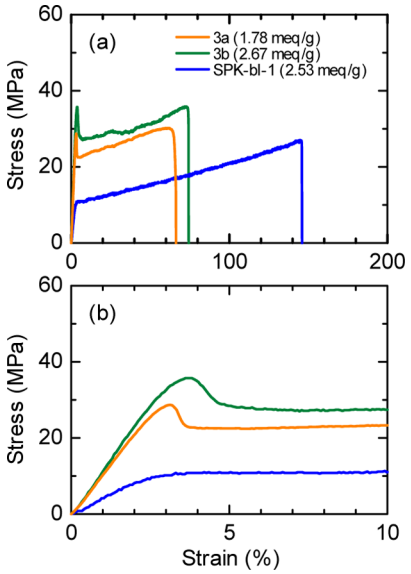

Figure 3. (a) Stress vs strain curves and (b) their elastic regions of the **3** and SPK-*bl*-1 membranes at 80 °C and 60% RH.

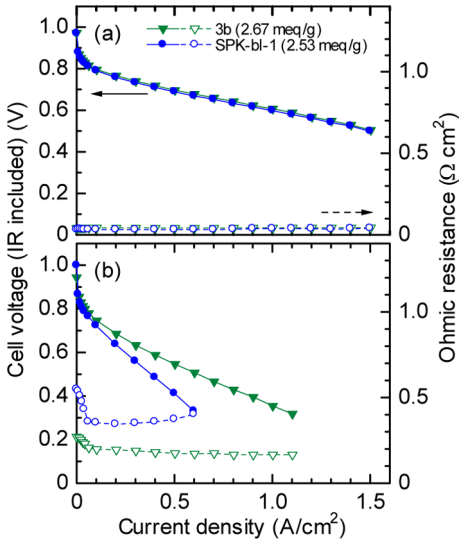

Figure 4. *IR*-included H_2/air polarization curves and ohmic resistances of the **3b** cell (2.67 mequiv/g, green inverted triangles) and SPK-*bl*-1-cell (2.53 mequiv/g, blue circles) at 80 °C under humidity conditions of (a) 100% and (b) 30% RH.

4b). The better fuel cell performance of the **3b** cell resulted from its lower ohmic resistance, reflecting the higher proton conductivity of the **3b** membrane at low RH.

In conclusion, we have investigated the effect of the sulfo-1,4-phenylene unit as a hydrophilic component on the properties of aromatic ionomer membranes. Due to the absence of polar groups such as ether, ketone, or sulfone groups in the hydrophilic component, the title **3** membranes exhibited reduced water uptake and excellent mechanical stability under humidified conditions. The high local IEC (ion concentration) in the hydrophilic segments contributed to an increase in the proton conductivity, especially at low humidity. Consequently, high-IEC **3b** (2.67 mequiv/g) membrane exhibited high proton conductivity under both low humidity (20% RH, 7.3 mS/cm) and high humidity (90% RH, 330 mS/cm) conditions at 80 °C, which are some of the highest values reported thus far. The improved properties of the **3** membranes were confirmed in an operating fuel cell.

■ ASSOCIATED CONTENT

Supporting Information

Experimental details as well as supporting properties. The Supporting Information is available free of charge on the ACS Publications website at DOI: 10.1021/acsmacrolett.5b00385.

■ AUTHOR INFORMATION

Corresponding Author

*E-mail miyatake@yamanashi.ac.jp. Tel.: +81 552208707. Fax: +81 552208707 (K.M.).

Author Contributions

The manuscript was written with equal contributions of all authors.

Notes

The authors declare no competing financial interest.

■ ACKNOWLEDGMENTS

This work was partly supported by the New Energy and Industrial Technology Development Organization (NEDO) through the HiPer-FC Project and the Ministry of Education, Culture, Sports, Science and Technology (MEXT) Japan through a Grant-in-Aid for Scientific Research (26289254).

■ REFERENCES

(1) Hickner, M. A.; Ghassemi, H.; Kim, Y. S.; Einsla, B. R.; McGrath, J. E. *Chem. Rev.* **2004**, *104*, 4587−4612.
(2) Higashihara, T.; Matsumoto, K.; Ueda, M. *Polymer* **2009**, *50*, 5341−5357.
(3) Peckham, T. J.; Holdcroft, S. *Adv. Mater.* **2010**, *22*, 4667−4690.
(4) Park, C.-H.; Lee, C.-H.; Guiver, M. D.; Lee, Y.-M. *Prog. Polym. Sci.* **2011**, *36*, 1443−1498.
(5) Kreuer, K. D. *Chem. Mater.* **2014**, *26*, 361−380.
(6) Miyatake, K.; Chikashige, Y.; Higuchi, E.; Watanabe, M. *J. Am. Chem. Soc.* **2007**, *129*, 3879−3887.
(7) Tian, S.; Meng, Y.; Hay, A. S. *Macromolecules* **2009**, *42*, 1153−1160.
(8) Bae, B.; Yoda, T.; Miyatake, K.; Uchida, H.; Watanabe, M. *Angew. Chem., Int. Ed.* **2010**, *49*, 317−320.
(9) Li, N.; Wang, C.; Lee, S. Y.; Park, C. H.; Lee, Y. M.; Guiver, M. D. *Angew. Chem., Int. Ed.* **2011**, *50*, 9158−9161.
(10) Asano, N.; Aoki, M.; Suzuki, S.; Miyatake, K.; Uchida, H.; Watanabe, M. *J. Am. Chem. Soc.* **2006**, *128*, 1762−1769.
(11) Yin, Y.; Suto, Y.; Sakabe, T.; Chen, S.; Hayashi, S.; Mishima, T.; Yamada, O.; Tanaka, K.; Kita, H.; Okamoto, K. *Macromolecules* **2006**, *39*, 1189−1198.
(12) Yamazaki, K.; Kawakami, H. *Macromolecules* **2010**, *43*, 7185−7191.
(13) Ghassemi, H.; Ndip, G.; McGrath, J. E. *Polymer* **2004**, *45*, 5855−5862.
(14) Fujimoto, C. H.; Hickner, M. A.; Cornelius, C. J.; Loy, D. A. *Macromolecules* **2005**, *38*, 5010−5016.
(15) Goto, K.; Rozhanskii, I.; Yamakawa, Y.; Otsuki, T.; Naito, Y. *Polym. J.* **2009**, *41*, 95−104.
(16) Umezawa, K.; Oshima, T.; Yoshizawa-Fujita, M.; Takeoka, Y.; Rikukawa, M. *ACS Macro Lett.* **2012**, *1*, 969−972.
(17) Jouanneau, J.; Mercier, R.; Gonon, L.; Gebel, G. *Macromolecules* **2007**, *40*, 983−990.
(18) Chang, Y.; Brunello, G. F.; Fuller, J.; Hawley, M.; Kim, Y. S.; Disabb-Miller, M.; Hickner, M. A.; Jang, S. S.; Bae, C. *Macromolecules* **2011**, *44*, 8458−8469.
(19) Weiber, E. A.; Takamuku, S.; Jannasch, P. *Macromolecules* **2013**, *46*, 3476−3485.
(20) Elabd, Y. A.; Hickner, M. A. *Macromolecules* **2011**, *44*, 1−11.

DOI: 10.1021/acsmacrolett.5b00385
ACS Macro Lett. 2015, 4, 750−754

(21) Miyahara, T.; Hayano, T.; Matsuno, S.; Watanabe, M.; Miyatake, K. *ACS Appl. Mater. Interfaces* **2012**, *4*, 2881−2884.
(22) Mochizuki, T.; Uchida, M.; Uchida, H.; Watanabe, M.; Miyatake, K. *ACS Appl. Mater. Interfaces* **2014**, *6*, 13894−13899.

DOI: 10.1021/acsmacrolett.5b00385
ACS Macro Lett. 2015, 4, 750−754